Outstanding shortening of the activation process stage for a TiFe-based hydrogen storage alloy

Ali Zeaiter[a, *], Philippe Nardin[a], Mohammad Arab Pour Yazdi[b], Alain Billard[b]

[a] *Univ. of Bourgogne Franche-Comte, Femto-ST UMR CNRS 6174, Department of Applied Mechanics, FCLAB FR CNRS 3539, 24 rue de l'Epitaphe, Besançon, France*
[b] *Univ. of Bourgogne Franche-Comte, Femto-ST UMR CNRS 6174, MN2S department, FCLAB FR CNRS 3539, 15B Avenue des Montboucons, 25000, Besançon, France*

A B S T R A C T

Hydrogen solid storage in intermetallic compounds has attracted great attention in the recent decades; TiFe-based metal hydride is one of the most important candidate materials to hold atomic hydrogen because of its significant storage capacity (about 1.9 wt. %) and its moderate operating pressure and temperature. The main hindrance to an effective and large use of this metal forming hydride is the difficult activation process i.e. the initial hydriding attempt. In this paper an experimental study about the first hydrogenation process of $TiFe_{0.9}Mn_{0.1}$ is carried out with a Sievert apparatus. At first, powder fabrication protocol then materials and methods used for the experimental characterizations are described. Secondly, a literature survey is presented about the activation processes of TiFe based alloys. Finally experimental results, discussions and conclusions are exposed. Those results lead to a comparison between the hydrogenation behaviors of two $TiFe_{0.9}Mn_{0.1}$ powder types: the 'as received' powder and the same powder after a thermo-chemical treatment. A wide improvement in the hydrogen activation response is noticed when the powder is submitted to this thermo-chemical treatment under specific operating conditions of gas pressure, temperature and time-duration. Plotted PCI curves and XRD patterns demonstrate that the material bulk is not affected by this thermo-chemical treatment. Then, the operating conditions are optimized, and SEM visualizations are performed in order to point out the effects of the treatment on the surface properties of $TiFe_{0.9}Mn_{0.1}$ particles. At the end, a conclusion summarizes the main results and outlines the perspectives of such thermo-chemical treatment.

1. Introduction

Facing environmental and economic problems related to greenhouse gas emissions and depletion of fossil fuels, hydrogen gas associated to renewable energies appears as one of the best solutions to promote. It represents a green energy vector due to its combustion that produces only water vapor and heat.

The hydrogen energy sector is composed of three main areas: production, storage and distribution. The hydrogen storage methods concentrate the main problems and challenges.

Traditionally, hydrogen gas is stored by two ways: compressed gas [1] and liquid hydrogen at 20 K under atmospheric pressure [2]. The volumetric density of hydrogen is only 42 kg_{H2}/m^3 under 700 bar in compressed form, but for liquefied form, it increases up to 70 kg_{H2}/m^3. Given the limitations of these two traditional ways of storing hydrogen (density issue, high energy necessary, sophisticated tanks and boil off),

the solid storage method appears as an alternate way. This method is based on the solid-gas interaction principle: adsorption-absorption process [3]. Intermetallic compounds allow a reversible storage corresponding to phase change in the material. Many types of intermetallic compounds can be listed such as A, AB, AB_2, AB_5, A_2B_7, Zr-Fe-V, RE-Mg-Ni based alloy [4–8] … Each material is characterized by its maximum hydrogen storage capacity and its operating conditions of pressure and temperature. These two characteristics are gathered in Pressure-Composition-Isotherm curves (PCI) [9].

Main advantages of the hydrogen solid storage in intermetallic compounds concern safety and potential savings. For example, the operating conditions of temperature and pressure for hydrogen storage in $TiFe_{0.9}Mn_{0.1}$ are 25 °C and 5.8 bar respectively [10]. They are far away from the extreme conditions of compressed gas or cryogenic storage methods and lead to a safe use of a compact tank especially for transportation applications.

* Corresponding author.
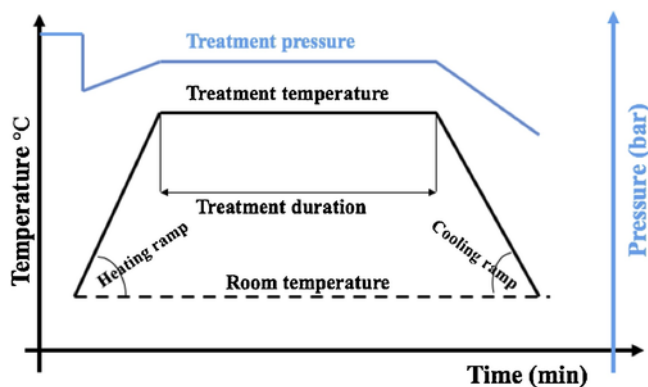*Email address:* alizeaiter32@gmail.com (A. Zeaiter).

Fig. 1. Schematic diagram of the performed thermo-chemical treatment.

Among many intermetallic compounds, an AB type TiFe is considered as an interesting candidate for hydrogen solid storage due to the abundance of its raw materials, its good storage capacity of 1.9 wt.% [11] corresponding to 120 kg_{H2}/m^3 coupled with moderate plateau pressures (10 and 4 bar for absorption/desorption respectively [11]), moderate enthalpy of hydride formation and good absorption/desorption kinetics.

In order to ensure a reliable development of such an intermetallic compound through an industrial scale, hydrogenation performances must be enhanced. The hydrogenation performances are defined as: easy activation process, high absorption/desorption kinetics and a good storage capacity. Typically, the activation process includes two parts: the first part is called the incubation time and the second part is related to the first actual absorption stage. An efficient material must have the shorter duration for these two parts.

TiFe is known to have a very difficult activation process [12–14] and a high sensitivity to impurities [15]. As reported in the literature, the substitution of iron by a small amount of manganese, aluminum or nickel facilitates the activation process [16–18]. Generally, any element with higher oxide stability, promote the activation of TiFe. In particular, manganese can chemisorb hydrogen and produce a marked enhancement of the activation [16,19]. However, the activation process of this intermetallic is still a challenge to overcome and therefore the AB_5 type $LaNi_5$ represents about 80% of the whole metal hydrides in the commercial market.

In this study, we focus on the activation process of an AB type TiFe based alloy powder whose stoichiometric formula is $TiFe_{0.9}Mn_{0.1}$ (substitution of Fe by 10% of Mn). The production method and characterization protocol will be described. The activation curve will be presented and a treatment to accelerate the activation process will also be discussed with its resulting effects.

2. Materials and methods

The hydride forming material used in this study is produced by high frequency induction furnace. Based on its chemical composition ($TiFe_{0.9}Mn_{0.1}$) and for one unit of mass, the theoretical weight proportions of Ti, Fe and Mn are respectively: 46, 48.4 and 5.6%. Those elements are put together in a crucible surrounded by a solenoid, and melted in ultra-high vacuum. A cooling circuit is integrated to the furnace, in order to evacuate heat and ensure the homogeneity of the temperature inside the crucible. At the end of the production stage the ingot is crushed into small pieces using a jaw crusher under nitrogen atmosphere and then sieved to a particle size of less than 100 μm. To reduce the surface oxidation the resulting powder is conserved in vacuum bags. Later, that manufactured intermetallic powder is called 'as received' powder.
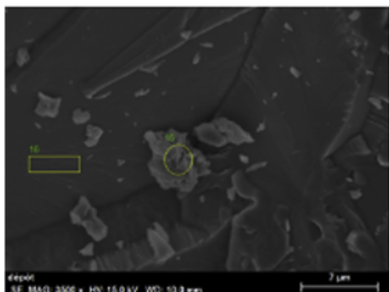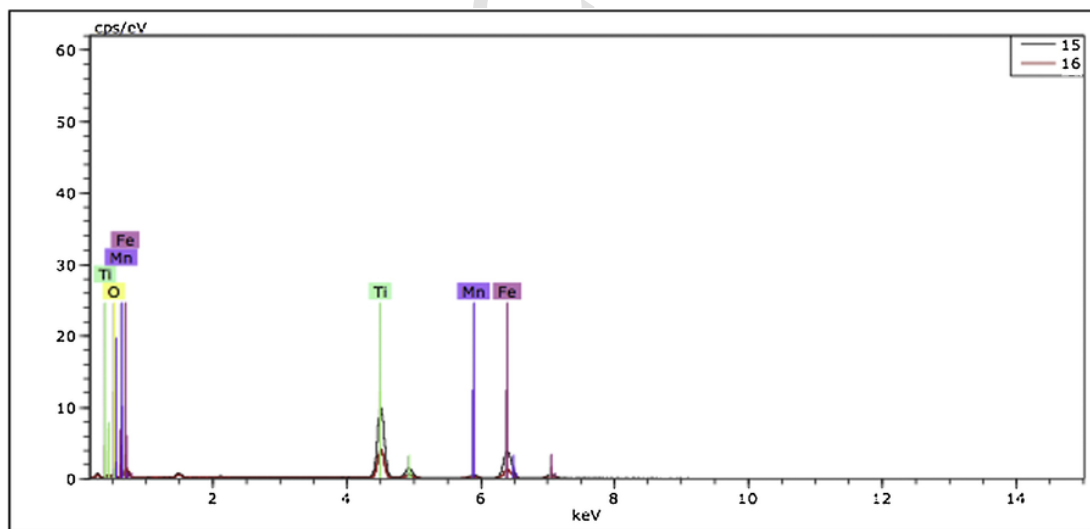

Fig. 2. Pattern from local EDS measurement on TiFe0.9 Mn0.1 'as received' powder.

Table 1
Weight percentages of present atoms calculated from an EDS measurement.

Weight % (Error < 1%)				
Element	O	Fe	Ti	Mn
15 (O included)	3.7	47.62	44.57	4.11
15 (Without O)	–	49,44	46,28	4,26

Afterwards, the 'as received' powder is considered for activation process and Pressure-Composition-Isotherm identification (i.e. thermo-dynamic characterization). Such a characterization is carried out using the Sievert method (manometric measurements) by means of an IMI HIDEN ISOCHEMA system. This system is suitable for a measuring range from 25 mbar to 200 bar coupled with a fine temperature control (+ 0.01 °C) inside the reactor between −25 and 500 °C

A widely used procedure for activation of the 'as received' powder consists of applying alternative cycling between a high pressure of hydrogen gas (40 bar) and a primary vacuum at room temperature (25 °C): 250 min for the high pressure of hydrogen followed by 150 min for the primary vacuum. Next to the activation stage, a PCI curve is measured at 22 °C.

On the other hand, and by using the technical capacities of the IMI HIDEN ISOCHEMA system, another fresh sample of the same 'as received' powder batch undergoes an in-situ thermo-chemical treatment prior to activation stage. During this treatment the sample is heated to a high temperature (from 300 to 400 °C) under a high pressure of hydrogen atmosphere for a predefined time. Subsequently, the treated sample is activated at 25 °C, and PCI curve is measured at 22 °C. Fig. 1

displays a schematic drawing illustrating the principle of the thermo-chemical treatment.

Morphological properties of the powders were evaluated by surface observations with a JEOL JSM-7800 F field emission scanning electron microscope (FE-SEM) and the chemical composition of the studied powders was confirmed by energy dispersive spectroscopy (EDS). In addition, X-ray diffraction measurements are also realized for structural characterization in Bragg-Brentano configuration by using a BRUKER D8 focus diffractometer with a cobalt X-ray tube equipped with a Lynx-Eye linear detector. Patterns were collected under airflow during about 13 min in the 20-100° angle range at a scan rate of $0.1°s^{-1}$.

In section below and before discussing our results, a literature survey is presented on previous works concerning the TiFe activation process

3. TiFe based alloys activation process

The activation process of TiFe is related to surface issues. The adsorbed hydrogen penetrates into the surface before being dissolved in the material bulk. The limiting step of the activation mechanism is controlled by surface properties of the hydride forming material. It is well known that for transition metals, clean surface promotes the dissociation process of the molecular hydrogen gas and enhances the overall activation mechanism [20]. Essential action to perform when proceeding to activate an intermetallic material is surface cleaning, and therefore removing the passivating oxides layers.

Based on literature survey, many publications concern the activation process of TiFe, or TiFe based alloys. Zhu et al. [21] have acti-
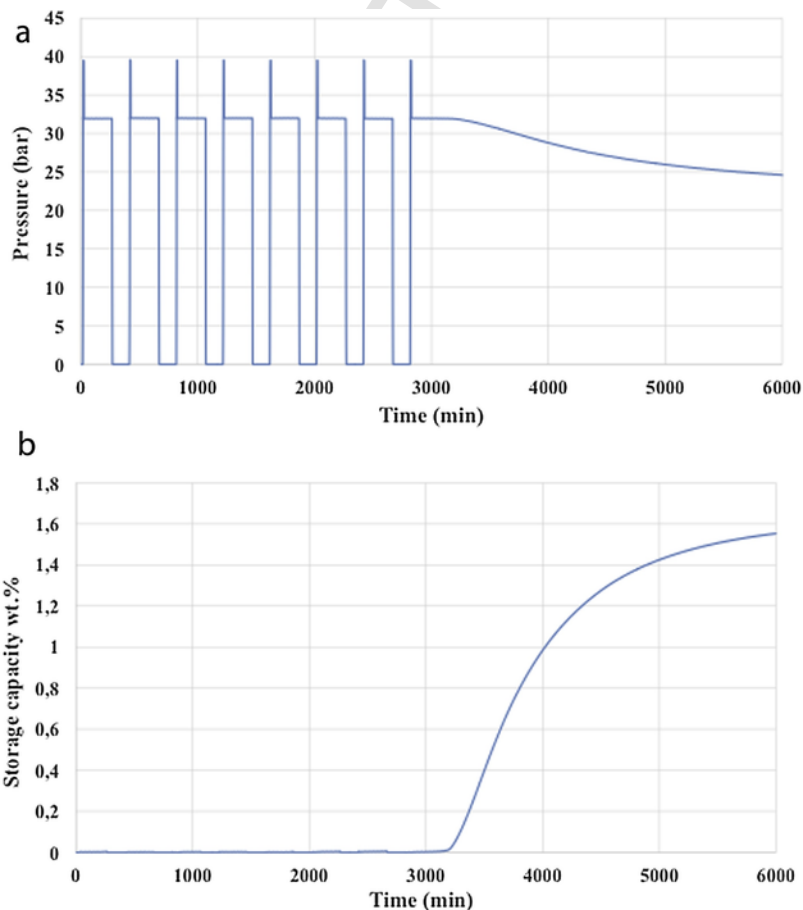

Fig. 3. 'As received' powder activation profiles according to time: a) Pressure profile, b) H2 storage capacity profile.
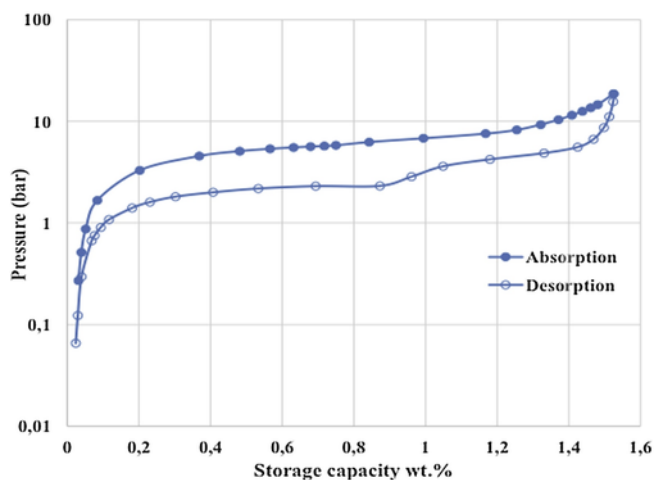
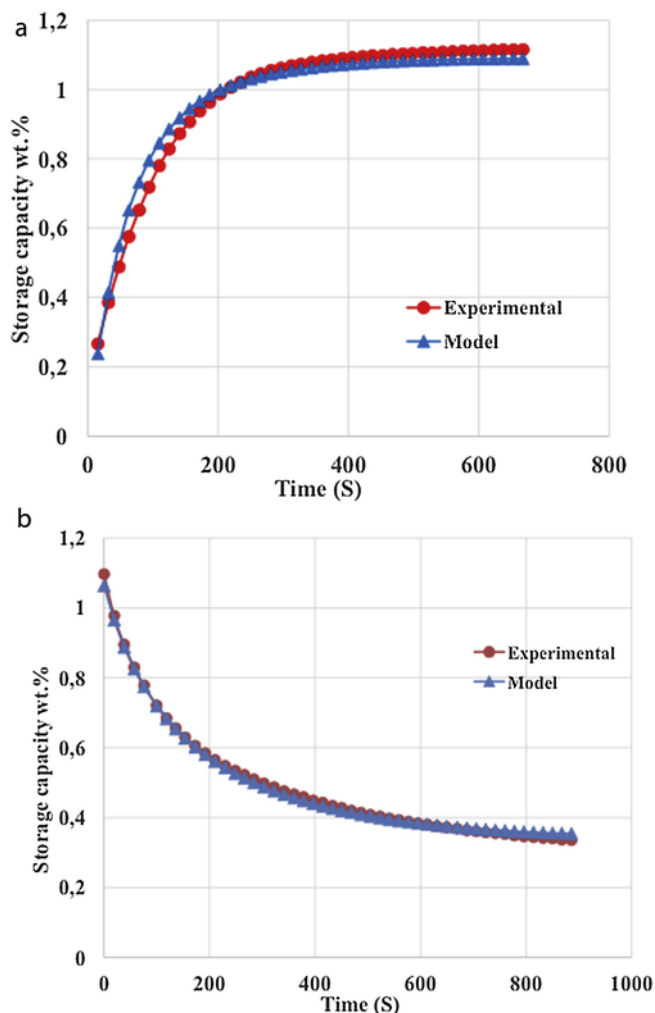**Fig. 4.** PCI curve for the as received powder at 22 °C.

Fig. 5. Curve fitting between experimental and theoretical data for a) absorption and b) desorption.

Table 2
Identified parameters for TiFe0.9Mn0.1 (activation energies and pre-exponential factors).

$TiFe_{0.9}Mn_{0.1}$	
Absorption	Desorption
$E_a = 19{,}43 \pm 2{,}52$ kJ/mole	$E_d = 18{,}70 \pm 0{,}54$ kJ/mole
$C_a = 43{,}43 \pm 0{,}6$ 1/s	$C_d = 22{,}77 \pm 0{,}1$ 1/s

Table 3
Identified parameters for LaNi5 hydride powder (activation energies and pre-exponential factors).

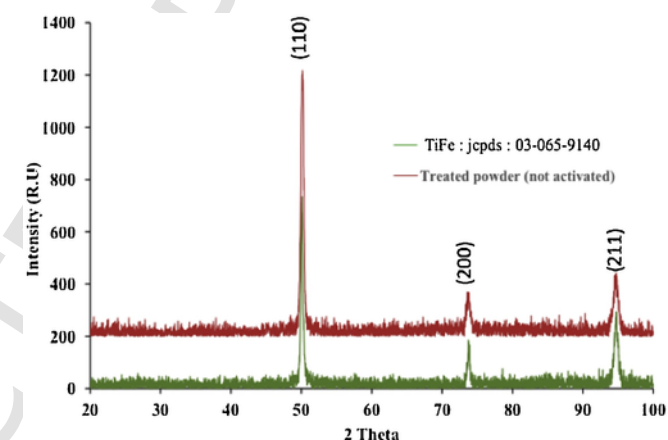| $LaNi_5$	
Absorption	Desorption
$E_a = 20.78 \pm 1.42$ kJ/mole	$E_d = 16.34 \pm 0.85$ kJ/mole
$C_a = 60.03 \pm 0.32$ 1/s	$C_d = 9.81 \pm 0.23$ 1/s

Fig. 6. XRD patterns for the 'as received' and treated powder.

nealing under 7 atm of hydrogen pressure during 30 min [12]. Moreover Sandrock et al. [23] mention that TiFe air crushed samples are covered by 20–30 nm thick oxygen rich film, which seems to prevent the molecular hydrogen to be adsorbed on the surface under ambient temperature. When the sample is exposed to high temperature, this thick rich oxygen film is made clear to dihydrogen and absorption reaction is initiated [23]. Schlapbach et al. [24] [25] reported that, when an intermetallic react easily with molecular hydrogen, it presents a tough oxygen induced surface segregation. This segregation protects the surface from the formation of passivating oxide layers and set up active sites for the dihydrogen dissociation. For TiFe, the segregation phenomena do not occur in normal conditions of pressure and temperature, and a heat treatment is necessary to ensure it: Ti diffuses to the surface and oxidizes, and the residual Fe forms a superparamagnetic precipitate that is responsible of molecular hydrogen dissociation [26]. Other research activities were also conducted by Kulshreshtha et al. [27]. They also reported that the activation behavior is related to the surface properties of the material. They have demonstrated that heating a pure TiFe sample in an oxygen atmosphere followed by a heat treatment at 625 K under hydrogen flow for several hours is very effective to create iron clusters and to dissociate the dihydrogen molecules. Kim H et al [28] described the chemical reactions that should occur on TiFe particles. Waldkirch et al. [29] agreed with this segregation mechanism [28], and suggested that after annealing of TiFe in vacuum or in hydrogen, surface precipitates of Fe are formed which inhibit the formation of oxide layers and facilitate the diffusion of hydrogen into the material core. Instead Fruchart et al. [30] proposed that a second phase

vated an arc melted TiFe sample by performing a 30 times pressure cycling (0.01 to 40 bar) at room temperature, for a duration of 20 min. This process contributes to surface cleaning and promotes the reactivity of molecular hydrogen gas with hydride forming material as it was also reported by Latroche [9] and Massicot [22]. Reilly and Wiswall reported that TiFe is activated after heating at 670 K in vacuum and an-
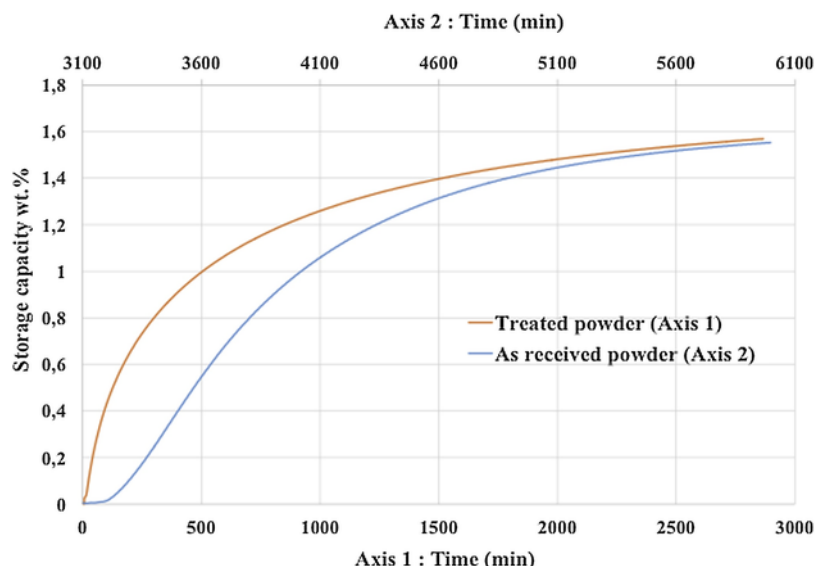
Fig. 7. Activation curves comparison for the 'as received' and treated powder.
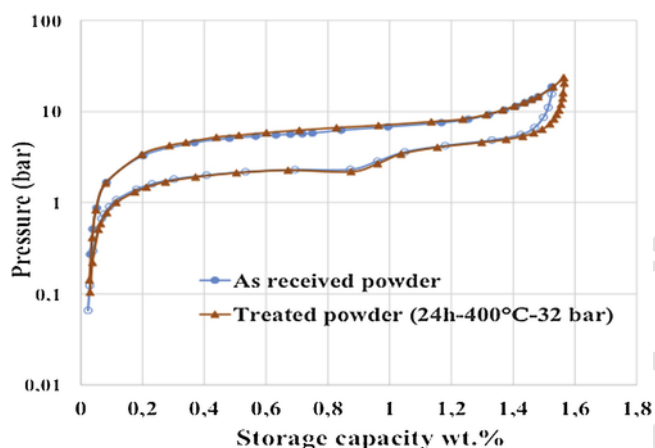

Fig. 8. PCI curves comparison between the 'as received' and treated powders.

$Fe_2Ti_4O_x$ acts as an activation promotor for the heat-treated TiFe, but they doubted about the catalytically effect of Fe precipitates. Schober et al. [31] have also refuted the concept of creating iron clusters after

heating. They have proposed another mechanism for the activation reaction: heating TiFe in vacuum leads to the formation of a catalytically active surface as the result of dissociation of the original oxide layers into the TiFe matrix. And another catalytic activity comes from n-TiO_2 that are in epitaxial contact with the TiFe matrix. Simultaneously Fe_2Ti clusters are formed, which are also responsible of the easy activation for Kulshreshtha et al. [32].

Shenzhong et al. [16] have treated a powder of $TiFe_{0.9}Mn_{0.1}$ prior to the activation stage. They proposed the following treatment protocol: cleaning surface with bombardment by argon ions, cycling under ultra-high vacuum at temperatures of 100 °C and 200 °C for a duration of 10 min and 30 min. The treated powder is then subjected to hydrogen pressure, and the activation process is initiated. The authors proposed a mechanism for the activation reaction: Manganese (Mn) aggregates at the surface of the particles, and assemble with titanium (Ti) to form TiMn molecule. TiMn reacts with hydrogen and forms entry points for diffusion to the core

Whatever the proposed mechanism for activation, all these previous studies agreed that a dedicated treatment is necessary to improve the activation process of TiFe based alloys.
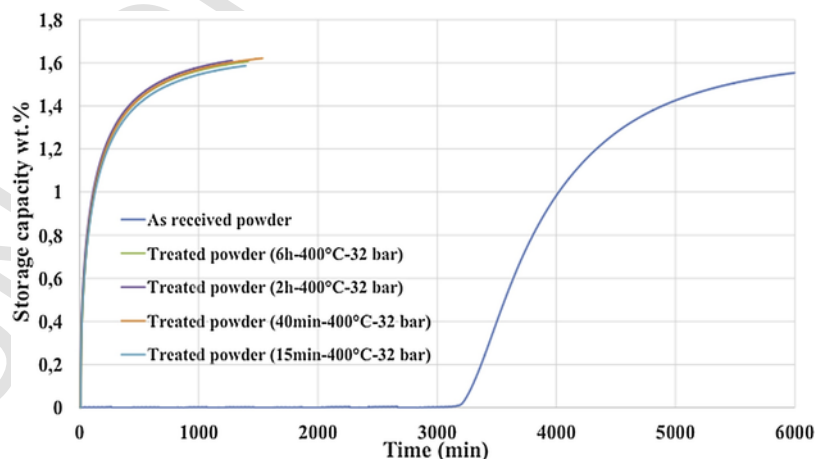

Fig. 9. Activation curves comparison for different thermal treatment durations.
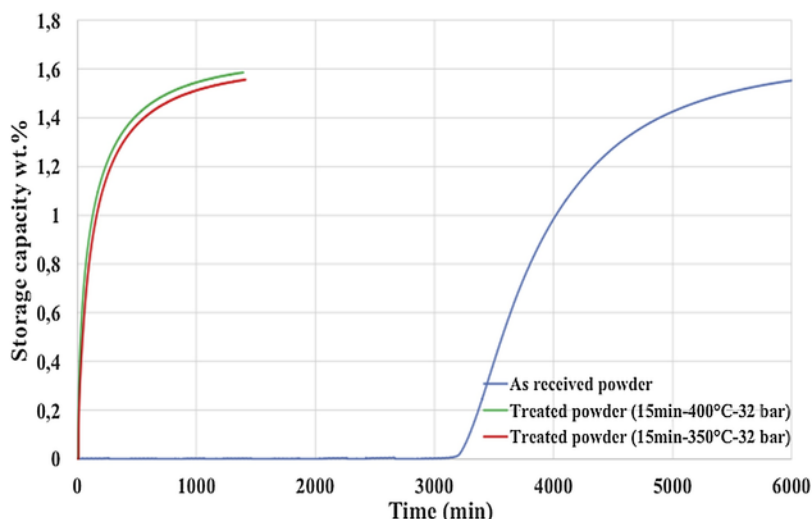
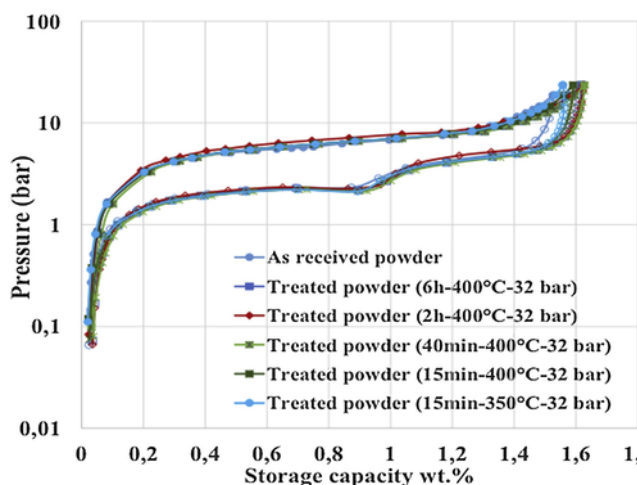**Fig. 10.** Activation comparison for different heating temperatures.

Fig. 11. PCI curves comparison for different operating conditions of the 'ZN' tests series.

4. Results and discussions

4.1. Chemical composition

After material powder being produced, EDS measurements are made to confirm its chemical composition, two zones have been chosen on the SEM image (Fig. 2) for this measurement. They are identified by the numbers 15 (on a homogeneous main face of a representative particle) and 16 (on another particle of much smaller dimensions). Table 1 summarizes the weight percentages of the existent elements for zone 15 of an effective particle. The measurement volume is about $1\,\mu m^3$.

From the calculated weight percentages, a comparison can be established between the theoretical and actual chemical composition. The presence of the oxygen element with a significant percentage indicates oxidation, which has occurred on the surface during the manufacturing and handling of the powder. Since oxygen element is not part of the initial chemical composition of the alloy powder, the real percentages of elements Fe, Ti and Mn are recalculated. They are very close to the theoretical composition (see § 2).
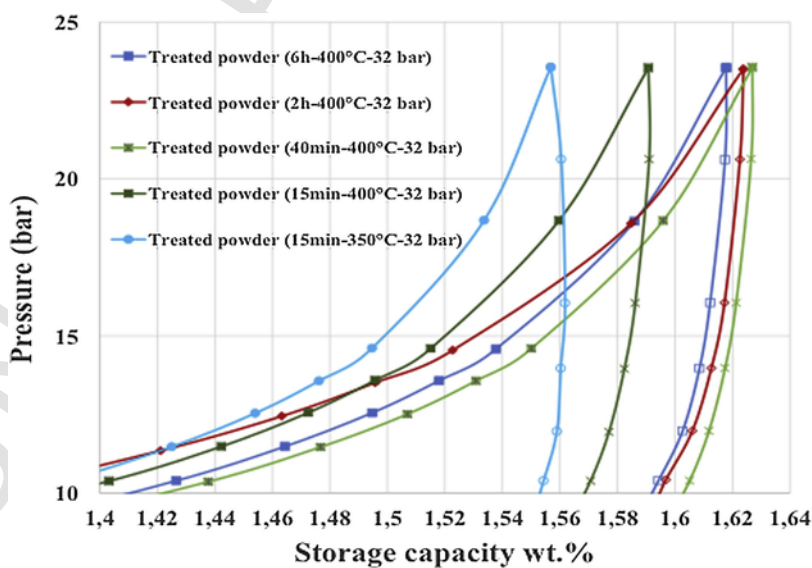

Fig. 12. Magnification of the measured PCI curves of the treated samples.

Table 4

Recapitulative table for the total activation time, the shortening time percentage and the maximum storage capacity for the ordinary activated 'as received' and treated powders.

Sample identification	Total time of activation (min)	Gain percentage (%)	Maximum storage capacity (wt. %)
Ordinary activated powder	6000	–	~1.55
Treated powder (6 h-400 °C)	1980	67	~1.61
Treated powder (2 h-400 °C)	1740	71	~1.62
Treated powder (40min-400 °C)	1620	73	~1.63
Treated powder (15min-400 °C)	1595	73.4	~1.59
Treated powder (15min-350 °C)	1595	73.4	~1.55
Treated powder (15min-300 °C)	6000	0	~1.55

4.2. 'Ordinary' activation process

Following EDS measurements, the 'as received' powder is considered for activation. A fresh sample (from 3 to 4 g) is filled into the reactor cell. Then an initial hydrogen pressure of 40 bar is applied in the dosing volume of the IMI HIDEN ISOCHEMA system at 25 °C, the hydrogen gas pressure falls down to 32 bar after expansion in the reactor cell. During the first 250 min, the powder does not exhibit any reaction with the hydrogen gas (a constant pressure profile is measured), consequently a primary vacuum is applied for 150 min in order to clean particles' surfaces and facilitate the activation process. This cycling: 250 min exposition under 32 bar of hydrogen pressure followed by 150 min of primary vacuum (25 mbar) is repeated seven times until the real be-

ginning of the absorption reaction. Fig. 3 shows the activation curves of the 'as received' powder: pressure and hydrogen storage capacity profiles versus time.

The incubation time lasts approximatively 3100 min, as shown in Fig. 3. Thereafter the hydrogen pressure in the reactor exhibits a decreasing profile corresponding to a significant absorption rate (Fig. 3b). The total time of the activation process is divided into two parts: 3100 min as incubation time and 2900 min as absorption time. That is to say, it needs about 6000 min to achieve the activation process (final capacity: 1.55 wt. %).

Next to powder activation a PCI curve at 22 °C is carried out with increasing pressure doses from 0.01 to 20 bar as displayed on Fig. 4.

This PCI curve at 22 °C is validated by previous work in the literature [10]. It indicates an absorption equilibrium pressure of 5.8 bar at the half of the hydrogen storage capacity (0.775 wt. %), where the absorption stage appears to take place with one single slightly sloping plateau. Contrariwise, desorption reaction comes in two stages: the phase transformation from γ to α occurs by passing through an intermediate β phase. These observations were also reported for annealed binary TiFe compounds [33,34]. This hydride forming material has a significant storage capacity, which reaches 1.55 wt. % and exhibits an interesting desorption equilibrium pressure (2.3 bar for the second phase). It is a valuable characteristic for use in practical applications such as coupling with a PEM fuel cell.

Following the measurement of PCI curve, several cycles of hydrogen absorption and desorption are carried out on the 'as received' powder. Afterwards, the generated experimental data are used to evaluate the activation energy of the powder through a fitting procedure. This procedure is based on the root mean square minimization method. The function to be minimized is (Eq.1):

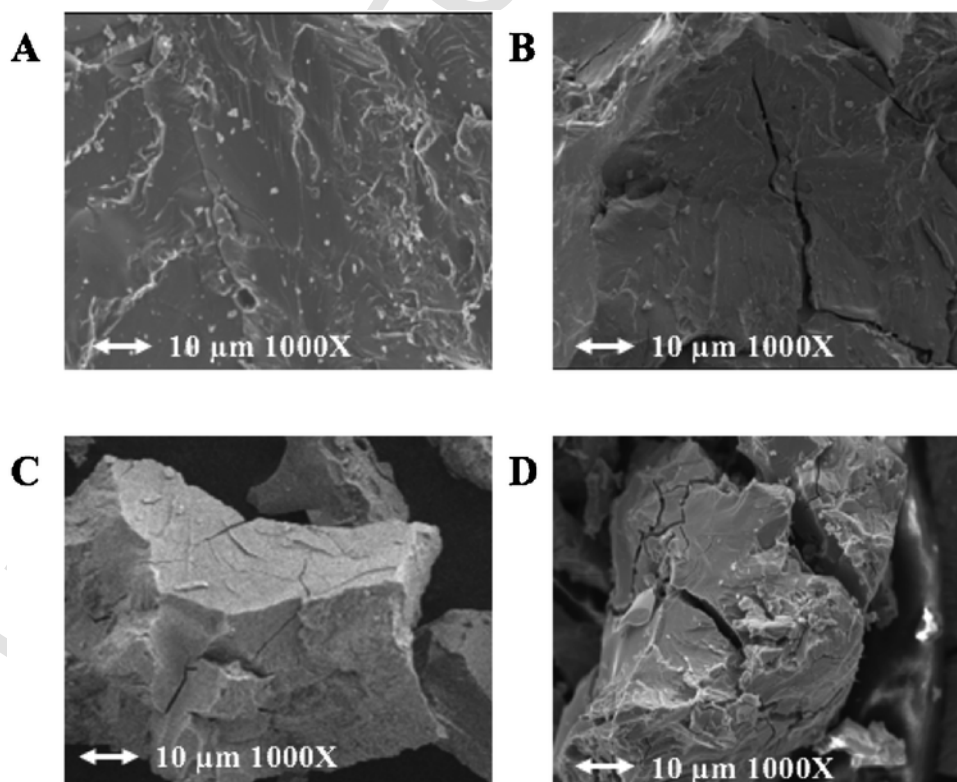$$\sum (Cm_{th} - Cm_{exp})^2 \qquad (1)$$

Where:

Fig. 13. Comparison of surface properties for: A) As received powder, B) Treated powder, C) 'as received' powder after ordinary activation, D) Treated powder after activation.

Cm_{th} represents the theoretical absorption/desorption hydrogen storage capacity (wt.%) versus time

Cm_{exp} represents the experimental absorption/desorption hydrogen storage capacity (wt.%) versus time

The hydrogen storage capacity (Cm_{th} or Cm_{exp}) is related to the rate of reaction. One of the most widely used theoretical model to describe hydriding/dehydriding reaction rate is presented in Eq. 2.a and Eq. 2.b

$$R_a(t) = C_a \exp\left(\frac{-E_a}{RT}\right) \ln\left(\frac{P_a}{P_{eq}}\right)\left(1 - \frac{m_{MH}}{m_s}\right) \qquad \text{absorption case} \quad (2.a)$$

$$R_d(t) = C_d \exp\left(\frac{-E_d}{RT}\right) \ln\left(\frac{P_d - P_{eq}}{P_{eq}}\right)\left(\frac{m_{MH}}{m_s}\right) \qquad \text{desorption case} \quad (2.b)$$

Where:

$R_a(t)$ represents the rate of the hydrogen absorption ($\frac{g_{MH}}{g_{m_s}S}$)

$R_d(t)$ represents the rate of hydrogen desorption($\frac{g_{MH}}{g_{m_s}S}$)

C_a, C_d are the pre-exponential factors of the Arrhenius law($\frac{1}{S}$)

E_a, E_d represent the activation energy for absorption and desorption respectively($\frac{kJ}{mol_{H_2}}$)

T is the operating temperature(K)

P_a, P_d represent the applied pressure during absorption and desorption respectively (Pa)

P_{eq} represents the equilibrium pressure in absorption/desorption(Pa)

m_s represent the dry mass of the hydride powder (non-hydrogenated)(g)

m_{MH} represents the hydride mass during absorption or desorption(g)

m_{MH} can be calculated through Eq. 3:

$$\frac{dm_{MH}}{dt} = R_{\frac{a}{d}}(t)m_s \qquad (3)$$

Then, the storage capacity in the theoretical case is calculated through Eq.4:

$$Cm_{th} = \frac{m_{MH}}{m_s}\frac{MW_{H_2}}{MW_{MH}} \times 100 \qquad (4)$$

The storage capacity in the experimental case is calculated through the generated absorbed/desorbed micro-mole numbers by the IMI system (N_{H_2}) (Eq. 5)

$$Cm_{exp} = \frac{N_{H_2} \times 10^{-6} \times MW_{H_2}}{m_s} \times 100 \qquad (5)$$

MW_{H_2} and MW_{MH} represent the molar mass of the hydrogen gas and hydride powder respectively.

After calculating the theoretical and experimental values of the hydrogen storages capacities, the minimization procedure uses MATLAB and excel simultaneously. Fig. 5 represents the adjusted fitted curves in case of absorption and desorption. The minimization procedure is repeated for 12 absorption/desorption cycles. The so identified parameters values are gathered in Table 2.

In order to validate our fitting procedure, we performed the same work on the LaNi$_5$ hydride powder (12 cycles of absorption/desorption). The activation energies and pre-exponential factors are identified (Table 3). They fully agree with the results reported by Talaganis et al. [35]

4.3. Activation after thermo-chemical treatment

In parallel, a fresh sample of the same batch of the 'as received' powder is filled into the reactor cell. This sample is subjected to a thermal treatment between 300 and 400 °C under a high pressure of hydrogen gas atmosphere prior to any H$_2$ absorption attempt. This high temperature range aims to promote the chemical reaction of dihydrogen on the surface oxides layers. This thermo-chemical treatment is further abbreviated as 'ZN' for simplification reasons. The first operating conditions of the 'ZN' treatment were:

- 24 h of treatment duration
- Heating temperature of 400 °C
- 32 bar of hydrogen pressure in the reactor cell
- Heating/cooling ramp of 4 °C/min.

The overall duration of the treatment was 27 h (1.5 h to reach the target heating temperature and the same time for the cooling process). Next to the treatment step, the powder is considered for XRD measurement. A comparison is made in Fig. 6 between XRD patterns for both powders (as received and treated). For the as received powder, principal diffraction peaks can be indexed in the CsCl-type structure with lattice parameters within the range $a = 2.990 \pm 0.003$ Å. After the thermo-chemical treatment process, the diffraction peaks kept the same positions and the same widening (no broadening was observed). This result confirms that thermo-chemical treatment does not change the structural properties of the material.

From the same batch of the 'as received' powder, another fresh sample is treated (24 h-400 °C-32 bar), and immediately activated. Applied pressure and temperature of the activation stage, are the same as for the ordinary activation process. The treated powder reacts immediately with hydrogen, and presents an improved initial reaction rate as shown in Fig. 7. The important difference with the ordinary activation process is that the time - consuming alternative cycling is not required

For a better comparison of the effective first H$_2$ absorption stages, the incubation time for the 'as received' powder curve is removed in Fig. 7. The curve is shifted of 3100 min towards the origin. That is, the period of incubation is not plotted to keep only the effective absorption step. By comparing them with the same scale unit (500 min), it is obvious that for the treated powder absorption rate is improved and the hydride forming metal absorbs hydrogen from the first minutes. For both samples and after 500 min from the beginning of the absorption reaction, the storage capacity of the treated powder reaches 1 wt.%, while with ordinary activation process the powder has only absorbed 0.58 wt.%. This wide improvement in the hydride forming metal activation response can be mainly explained by the partial removing or change in the chemical composition of oxide layers on the particles surfaces which act as hydrogen barrier [23].

Fig. 8 shows a comparison between PCI curves of the treated powder and the previous one related to the ordinary activated powder (Fig. 4).

It can be clearly seen that 'ZN' treatment slightly increases the storage capacity of the ɣ phase and does not affect the thermodynamic characteristics of the hydriding/dehydriding reaction of the core material. Indeed, the same values are noticed for the equilibrium pressures. This results also confirm that the activation process is related only to particles' surfaces as reported by L. Schlapbach et al. [15]. The performed thermo-chemical treatment is more suitable for TiFe$_{0.9}$Mn$_{0.1}$ powder than a mechanical treatment (ball milling), that can strongly affect the crystalline structure (amorphisation) and consequently reduce the maximum storage capacity [36–38].

4.4. Optimization of 'ZN' thermal treatment conditions

In our study, we also proceed for the optimization of the operating conditions of the 'ZN' treatment. The conditions to be refined in this study are the heating temperature and the time of treatment. Reducing the treatment duration to its minimum value is our first goal. The heat-

ing temperature must also be reduced in order to make this treatment easier to achieve for practical applications like inside a real hydride tank.

We have carried out four other treatment durations: 6 h, 2 h, 40 min, and 15 min. For these tests the heating temperature and hydrogen gas pressure in the reactor cell were the same (400 °C and 32 bar). Fig. 9 displays the measured activation curves for the ordinary activated powder and for the different durations of the 'ZN' treatment.

The activation curves show that the improvement in the activation process of this intermetallic does not depend on the thermal treatment duration. We can conclude that heating the powder during 15 min at 400 °C and under 32 bar of hydrogen pressure is sufficient to improve widely the activation of $TiFe_{0.9}Mn_{0.1}$.

By fixing the stabilized heating duration at 15 min, we tested a heating temperature of 350 °C under the same hydrogen pressure (32 bar). As shown in Fig. 10, the activation curves at 350 °C and 400 °C are alike. A small difference is noticed in the maximum storage capacities.

The 'ZN' treatment lasts 195 min and the first hydriding stage 1400 min. Consequently, the time between the beginning of the treatment and the first complete hydriding stage is about 1595 min. This duration is considered as the total time of activation from 'as received' powder.

When testing a heating temperature of 300 °C during 15 min, the powder did not react with hydrogen immediately and the activation curve tends to be close to the ordinary activated powder one. From these tests, the optimized conditions of the 'ZN' treatment to improve the activation mechanism of the AB type $TiFe_{0.9}Mn_{0.1}$ are a treatment duration of 15 min at 350 °C under 32 bar of hydrogen pressure. For all the previous tests, PCI curves are plotted and shown in Fig. 11.

It is worth noting that, the maximum storage capacity is not the same for all treated samples. A magnification of the measured PCI curves is presented in Fig. 12. For a heating duration of 6 h, 2 h or 40 min at 400 °C the maximum storage capacity is around 1.62 wt.%. This value decreases to 1.59 wt. % when the heating duration is 15 min and even 1.55 wt. % if in addition the temperature is 350 °C. This result is fully consistent with the activation curve of the treated powder at 350 °C for 15 min, where the value of the maximum storage capacity is also 1.55 wt.%. This behavior can be explained, by the fact that 350 °C as 'ZN' treatment temperature or 15 min as treatment duration are not enough to totally clean the surface and presumably a few places in the material bulk are still not able to absorb hydrogen.

To summarize the huge influence of the 'ZN' treatment on the total activation time of the $TiFe_{0.9}Mn_{0.1}$ powder with particles size less than 100 μ m, a recapitulative table (Table 4) is presented. The total activation time and the shortening time percentage compared with ordinary activation process are displayed.

4.5. SEM images of particles' surfaces

In order to understand, the effect of the 'ZN' treatment on surface properties of $TiFe_{0.9}Mn_{0.1}$ 4 samples A, B, C and D are examined. Sample A is the 'as received' powder after fabrication process. Sample B is the treated powder (350 °C-15 min-32 bar) but not activated. Sample C is the 'as received' powder after the ordinary activation stage (i.e. first hydriding). Sample D is the treated powder under the same conditions as sample B and activated. All the samples are considered for scanning electron microscopy visualization (SEM). Fig. 13 shows a comparison between their SEM images.

Except for sample A, these SEM images clearly exhibit the creation of cracks at the surface of the particles which act as gates for a better diffusion of the hydrogen inside the material. For sample B, the surface between hydrogen gas and the material increases and consequently the total time of activation is reduced, but the density of cracks is limited.

The high gas pressure of this treatment lead to the formation of a solid solution of the hydrogen gas and thereafter to a possible embrittlement at the grain boundaries or at the microstructural defects when the pressure suddenly falls down leading to the creation of new exchange surfaces for hydriding/dehydriding [31]. This increase of the specific surface area of intermetallic particles will have a positive effect on the activation. It seems that for sample C the reduction of the oxides layers begins with alternative cycling then continues during the incubation time and lasts much longer due to the lower temperature. For sample D, the swelling/shrinkage during hydrogen absorption/desorption lead to enhance the powder embrittlement Therefore, the SEM images of samples C and D are very similar from each other like their PCI curves.

5. Conclusions and perspectives

In the current study, a thermo-chemical treatment is performed on a $TiFe_{0.9}Mn_{0.1}$ hydride forming material. A comparison of XRD patterns, activation and PCI curves has been conducted between the ordinary activated 'as received' and treated powders. The 'as received' powder needs approximately 6000 min to be activated under 32 bar of hydrogen gas pressure at 25 °C. The treated powder exhibits a huge improvement in the total time of activation. It is only 1595 min long with an improvement factor greater than 3.7. This treatment affects only particles surface but not the material bulk. Indeed, PCI curves and XRD patterns are identical.

The presented curves and results are the early experimental ones and many parameters and conditions still need to be optimized. The hydrogen gas pressure is one of the parameters to be refine so as the cooling ramp. The effect of quenching on solidification structure of the alloy could facilitate the paths for hydrogen to the bulk while reducing the 'ZN' treatment duration. To highlight the influence of high pressure, a thermo-chemical treatment was carried out at 7 bar of hydrogen pressure under 350 °C during 15 min, the activation time was nearly the same as for the ordinary activated powder. This result confirms a previous work reported by Reilly et al. At our best knowledge, no pre-activation process has ever been carried out at high temperature and high-pressure gas simultaneously.

'ZN' treatment has been successfully carried out on other compositions of TiFeMn alloys and even pure TiFe with approximately the same result on the total activation time. It also permits to regenerate the storage capabilities of $TiFe_{0.9}Mn_{0.1}$ hydride powder after a long period (over 10 months) of air exposure. This work will be the subject of a future paper.

Nevertheless, a complete physico-chemical study in-situ should be performed in order to identify the real mechanisms of the activation process of the TiFe based metal hydrides.

TiFe based alloys are eco-friendly materials. They contain no rare earth and can be fully recycled by re-melting at the end of their product life cycle. Moreover, from an economic point of view, TiFe based alloys are less than half price of $LaNi_5$ alloys and could provide an effective and safe storage solution to launch first hydrogen applications in everyday life.

References

[1] M. Hosseini, I. Dincer, G. Naterer, M. Rosen, Thermodynamic analysis of filling compressed gaseous hydrogen storage tanks, Int. J. Hydrogen Energy 37 (2012) 5063–5071.

[2] B. Bowman, L. Klebanoff. Hydrogen Storage Technology: Materials and Application. Chapter 3, page: 69-71.

[3]   M. Martin, C. Gommel, C. Borkhart, E. Fromm, Absorption and desorption kinetics of hydrogen storage alloys, J. Alloys Compd. 238 (1996), 193-01.

[4]   T.M. Kasper, R.J. Torben, A. Etsuo, W.L. Hai, Hydrogen - a sustainable energy carrier, Prog. Nat. Sci.: Mater. Int. 27 (2017) 34–40.

[5]   Z. Cao, L. Ouyang, L. Li, Y. Lu, H. Wang, J. Lui, D. Min, Y. Chen, F. Xiao, T. Sun, R. Tang, M. Zhu, Enhanced discharge capacity and cycling properties in high-samarium, praseodymium/neodymium-free, and low-cobalt A_2B_7 electrode materials for nickel-metal hydride battery, Int. J. Hydrogen Energy 451 (2015) 451–455.

[6]   Z. Cao, L. Ouyang, H. Wang, J. Liu, L. Sun, M. Felderhoff, M. Zhu, Development of Zr-Fe-v alloys for hydride hydrogen storage system, Int. J. Hydrogen Energy 41 (2016) 11242–11253.

[7]   L. Ouyang, Z. Cao, L. Li, H. Wang, J. Liu, D. Min, Y. Chen, F. Xiao, M. Zhu, Enhanced high-rate discharge properties of $La_{11.3}Mg_{6.0}Sm_{7.4}Ni_{61.0}Co_{7.2}Al_{7.1}$ with added graphene synthesized by plasma milling, Int. J. Hydrogen Energy 39 (2014) 12765–12772.

[8]   L. Ouyang, X. Yang, M. Zhu, J. Liu, H. Dong, D. Sun, J. Zou, X. Yao, Enhanced hydrogen storage kinetics and stability by synergistic effects of in situ $CeH_{2.73}$ and Ni in $CeH_{2.73}$-MgH_2-Ni nanocomposites, J. Phys. Chem. 118 (2014) 7808–7820.

[9]   M. Latroche, Structural and thermodynamic properties of metallic hydrides used for energy storage, J. Phys. Chem. Solids 65 (2004) 517–522.

[10] H. Nagai, K. Kitagaki, K. Shoji, Microstructure and hydriding characteristics of TiFe alloys containing manganese, J. Less-Common Metals 134 (1987) 275–286.

[11] J. Schefer, P. Fischer, W. Halg, F. Stucki, L. Schlapbach, A. Andresen, Structural phase transition of FeTi-deuterides, Mater. Res. Bull. 14 (1979) 1281–1294.

[12] J.J. Reilly, R.H. Wiswall, Formation and properties of iron titanium hydride, Inorganic Chem. 13 (1974) 13.

[13] H. Inui, T. Yamamoto, M. Hirota, M. Yamaguchi, Lattic defects introduced during hydrogen absorption-desorption cycles and their effects on P-C characteristics in some intermetallic compounds, J. Alloys Compd. 330 (2002) 117–124.

[14] J.Y. Lee, C.N. Park, S.M. Pysm, The activation process and hydriding kinetics of FeTi, J. Less-Common Metals 89 (1983) 163–168.

[15] L. Schlapbach, A. Seiller, Y. Stucki, Surface segregation in FeTi and its catalytic effect on the hydrogenation II: AES and XPS studies, Mater. Res. Bull. 13 (1978) 1031–1037.

[16] Y. Shenzhong, Y. Rong, H. Tiesheng, Z. Shilong, C. Bingzhao, A study of the activation of FeTi and Fe0.9TiMn0.1, Int. J. Hydrogen Energy 13 (1988) 433–437.

[17] G. Bruzzone, G. Costa, M. Ferretti, G.L. Olcese, Hydrogen storage in aluminum-substituted TiFe compounds, Int. J. Hydrogen Energy 6 (1981) 181–184.

[18] H.S. Chung, J.-Y. Lee, Effect of partial substitution of Mn and Ni for Fe in FeTi on hydriding kinetics, Int. J. Hydrogen Energy 11 (335) (1986).

[19] S.-M. Lee, T.-P. Perng, Effect of the second phase on the initiation of hydrogenation of TiFe1−xMx (M = Cr,Mn) alloys, Int. J. Hydrogen Energy 19 (1994) 259–263.

[20] L. Schlapbach, T. Riesterer, The activation of FeTi for hydrogen Absorption, J. Appl. Phys. A32 (1983) 169–182.

[21] H.Y. Zhu, J. Wu, Q.D. Wang, Disproportionation of $LaNi_5$ and TiFe in 4 Mpa H_2 at 300 °C, J. Alloys Compd. 185 (1992) 1–6, Jalcom 225.

[22] B. Massicot, Etude du système Fe-Ti-V et de ses applications au stockage de l'hydrogène. Thèse, 2009.

[23] G.D. Sandrock, J.J. Reilly, J.R. Johnson, Stateline Nevada, Proceeding of the 11th Intersociety Energy Conversion and Engineering Conference (1976), page 965.

[24] L. Schlapbach, A. Seiler, F. Stucki, P. Zürcher, P. Fischer, J. Schefer, How FeTi Absorbs Hydrogen Zeitschrift für Physikalische Chemie (Neue Folge) (Weisbaden), 1979, 117:205.

[25] L. Schlapbach, A. Seiler, F. Stucki, H.-C. Siegmann, Surface effects on the formation of metal hydride, J. Less-Common Metals 73 (145) (1980).

[26] F. Stucki, L. Schlapbach, Magnetic properties of LaNi5, FeTi, Mg2Ni and their hydrides, J. Less-Common Metals 74 (143) (1980).

[27] S. Kulshreshtha, R. Sasikala, K. Pushpa, K. Rao, R. Iyer, On activation of TiFe: surface effects, Mater. Res. Bull. J. 24 (1989) 545–550.

[28] H. Kim, J. Lee, The effect of surface conditions on the activation of TiFe, J. Less Common Metals 105 (1985) 247–253.

[29] Th. Von Waldkirch, R. Wessiken, H.-U. Nissen, L. Schlapbach, Paris, 3rd International Congress on Hydrogen and Materials (1982) C9.

[30] D. Fruchart, M. Commandré, D. Sauvage, A. Rouault, R. Tellgren, Structural and activation process studies of Fe-Ti-like hydride compounds, J. Less-Common Metals 74 (55) (1980).

[31] T. Schober, D. Westlake, The activation of TiFe for hydrogen storage: a different view, Scr. Mettal. 15 (1981) 913–918.

[32] S. Kulshreshtha, R. Sasikala, P. Suryanarayana, A. Singh, M. Iyer, Studies on hydrogen storage material FeTi: effect of Sn substitution, Mater. Res. Bull. 34 (1988) 333–340.

[33] J. Reilly, J. Johnson, J. Lynch, F. Reidinger, Irreversible effects in the FeTi-H systems, J. Less-Common Metals 89 (1983) 505–512.

[34] T. Schober, Transmission electron microscopy and neutron diffraction studies of FeTi-H (D), J. Less-Common Metals 74 (1980) 23–31.

[35] A. Talaganis, G. Meyer, P. Aguirre, Modeling and simulation of absorption-desorption cyclic processes for hydrogen storage-compression using metal hydrides, Int. J. Hydrogen Energy 36 (2011) 13621–13631.

[36] J. Ares, F. Cuevas, A. Percheron-Guégan, Mechanical milling and subsequent annealing effects on the microstructural and hydrogenation properties of multisubstituted LaNi5 alloy, Acta Mater. 53 (2005) 2157–2167.

[37] J. Harris, W. Curtin, M. Tenhover, Universal features of hydrogen absorption in amorphous transition metal alloys, Phys. Rev. B 36 (1987) 5784–5797.

[38] Yu Zadorozhnyy, G.S. Milovzorov, S.N. Klyamkin, M.Yu Zadorozhnyy, D.V. Strugova, M.V. Gorshenkov, S.D. Kaloshkin, Preparation and hydrogen storage properties of nanocrystalline TiFe synthesized by mechanical alloying, Progr. Nat. Sci.: Mater. Int. 27 (2017) 149–155.